

This is the accepted manuscript made available via CHORUS. The article has been published as:

Quantum-enhanced spectroscopy with entangled multiphoton states

Hossein T. Dinani, Manish K. Gupta, Jonathan P. Dowling, and Dominic W. Berry

Phys. Rev. A **93**, 063804 — Published 7 June 2016

DOI: [10.1103/PhysRevA.93.063804](https://doi.org/10.1103/PhysRevA.93.063804)

Quantum enhanced spectroscopy with entangled multi-photon states

Hossein T. Dinani¹, Manish K. Gupta², Jonathan P. Dowling², Dominic W. Berry¹

¹*Department of Physics and Astronomy, Macquarie University, Sydney, NSW 2109, Australia*

²*Hearne Institute for Theoretical Physics, Department of Physics and Astronomy, Louisiana State University, Baton Rouge, Louisiana 70803, USA*

Traditionally, spectroscopy is performed by examining the position of absorption lines. However, at frequencies near the transition frequency, additional information can be obtained from the phase shift. In this work we consider the information about the transition frequency obtained from both the absorption and the phase shift, as quantified by the Fisher information in an interferometric measurement. We examine the use of multiple single-photon states, NOON states, and numerically optimized states that are entangled and have multiple photons. We find the optimized states that improve over the standard quantum limit set by independent single photons for some atom number densities.

I. INTRODUCTION

The goal of quantum metrology is to obtain the most precise measurements possible with minimal resources [1]. Many types of high-precision measurement use a form of interferometry. In interferometers, the unknown parameter is imprinted as the relative phase between a superposition of states. Measurement of the output state, after quantum interference, gives information about the unknown parameter.

One particular example is optical interferometry with Mach-Zehnder interferometers. In this case, using N independent photons gives $1/\sqrt{N}$ scaling for the uncertainty of phase measurements, which is known as the standard quantum limit. However, using N entangled photons gives $1/N$ scaling for the phase uncertainty, which is often called the Heisenberg limit. This enhancement in sensitivity is of much importance in probing delicate systems such as atoms [2] and biological samples [3].

A well-known type of entangled states is NOON states [4, 5]. Although NOON states saturate the Heisenberg limit, they perform poorly in the presence of absorption [6, 7]. It is shown that states of the form $\sum_{k=0}^N \psi_k |N-k, k\rangle$, are less sensitive to loss than NOON states due to the presence of extra terms in the superposition [8–11]. Even with such states, the advantage over the standard quantum limit in phase estimation is reduced by loss. However, we can take advantage of the sensitivity of nonclassical properties of quantum states to absorption. The sensitivity of quantum coherence can be used efficiently to estimate absorption [12], and also estimate physical quantities that the absorption depends on.

In Ref. [13] a sub-shot-noise measurement of absorption is obtained using heralded single photons. In that work, a non-interferometric setup was used, where all the information is obtained from absorption, and the quantum enhancement results from sub-Poissonian statistics of single photons. According to the Kramers-Kronig relation, absorption is accompanied by a phase shift [14]. However, the information from the phase is only accessible if we take advantage of superposition and interfer-

ence.

In Ref. [15] optimal states for simultaneous estimation of loss and phase are found. Such states are of the form $\sum_{k=0}^N \psi_k |N-k, k\rangle$ with a large weight on the loss mode to improve the estimation of loss. Here, we find the optimal states of similar form to estimate a parameter that both loss and phase depend on.

The system we are considering here is an ensemble of atoms. We are interested in measuring a transition frequency of the atoms. If this ensemble is probed by a beam of photons, the absorption of photons, and phase shift imposed on the probe, both depend on the transition frequency of atoms. We consider a Mach-Zehnder interferometer with the atomic ensemble placed in one of the arms of the interferometer. We optimize over the state in the arms of the interferometer and find the state from which we obtain the maximum information about the atomic transition frequency.

II. INTERFEROMETRIC SCHEME

Consider a Mach-Zehnder interferometer, as shown in Fig. 1, with an ensemble of atoms placed in the upper arm of the interferometer. Here, we consider an ensemble of identical two-level atoms in the absence of Doppler broadening and dipole dephasing. This simple model gives a good qualitative description of the problem. Assuming that all atoms interact equally with the input quantum state and that there is no interaction between atoms, using the dipole and rotating-wave approximation the susceptibility of the ensemble is given by [16, 17]

$$\chi(\Delta) = \chi'(\Delta) + i\chi''(\Delta) = \frac{2\mathcal{N}\mu^2}{\hbar\epsilon_0} \frac{\Delta + i\gamma_s}{\Delta^2 + \gamma_s^2}, \quad (1)$$

where $\Delta = \omega - \omega_0$ is the detuning between ω_0 , the transition frequency of atoms, and ω , the frequency of input photons, γ_s is the spontaneous decay rate of the excited state, \mathcal{N} is the number density of atoms, μ is the electric dipole moment, \hbar is the reduced Planck constant and ϵ_0 is the vacuum permittivity. Details of the derivation of this susceptibility based on interaction of an ensemble of atoms with quantized light are given in Refs. [16, 17].

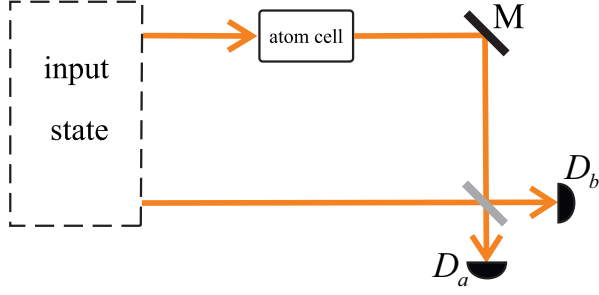


FIG. 1. A Mach-Zehnder interferometer with an ensemble of atoms placed in the upper arm. D_a and D_b are photon number detectors in the output modes.

The imaginary and real parts of the susceptibility are plotted in Fig. 2. In this figure we have used data for the D1 transition line of sodium from Ref. [18]; i.e. $\mu = 0.704 \times 10^{-29} \text{ C} \cdot \text{m}$ and $\gamma_s = 61.354 \times 10^6 \text{ s}^{-1}$. For the number density of atoms we have used $\mathcal{N} = 2.5 \times 10^{16} \text{ m}^{-3}$.

Knowing the susceptibility of the atomic medium, the effect of the atomic ensemble in the upper arm of the Mach-Zehnder interferometer can be modeled by the beam splitter model proposed in Refs. [19, 20]. Normally, one beam splitter is used to model loss in each of the arms of a Mach-Zehnder interferometer [9, 11, 21]. However, here we consider a line of n beam splitters, shown in Fig. 3 where each beam splitter represents one of the atoms in the ensemble. The k th beam splitter transforms the creation operator a_k^\dagger according to

$$a_k^\dagger = \sqrt{t(\omega)}a_{k+1}^\dagger + \sqrt{r(\omega)}b_k^\dagger, \quad (2)$$

where $t(\omega)$ and $r(\omega)$ are the transmissivity and reflectivity of the beam splitter, ω is the frequency of input photons, and b_k is the loss mode of the k -th beam splitter.

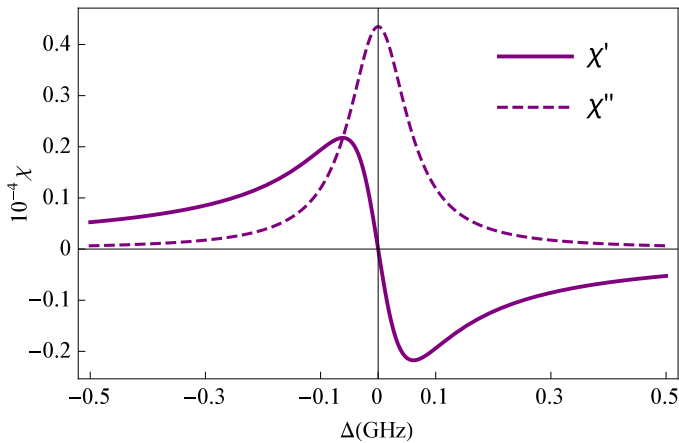


FIG. 2. The real (solid line) and the imaginary (dashed line) parts of susceptibility, χ' and χ'' respectively, calculated using Eq. (1) for the D1 transition line of sodium.

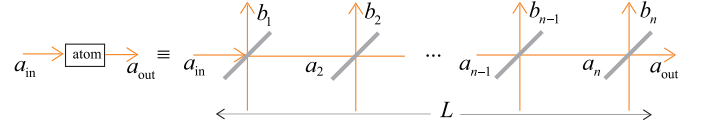


FIG. 3. Beam splitter model to model the interaction of photons with the ensemble of atoms.

The effect of the atomic ensemble is obtained by applying all the beam splitters, and taking the limit as the number of beam splitters approaches infinity. The creation operator of the input mode a_{in}^\dagger is therefore transformed to [19, 20]

$$a_{\text{in}}^\dagger = a_{\text{out}}^\dagger e^{-i\frac{\omega L}{c}\sqrt{1+\chi}} - i\sqrt{\frac{\omega}{c}\chi''} \int_0^L e^{-i\frac{\omega}{c}(L-z)\sqrt{1+\chi}} b^\dagger(z) dz, \quad (3)$$

where L is the length of the ensemble, ω is the frequency of the input photons, c is the speed of light and χ'' is the imaginary part of the susceptibility of the atomic ensemble $\chi = \chi' + i\chi''$. The real part of susceptibility, χ' , describes dispersion and the imaginary part, χ'' , describes absorption by the ensemble.

From Eq. (3), the transmissivity of the ensemble, T , and the phase shift imposed on the state from the ensemble, φ , can be written in terms of the imaginary and real parts of the susceptibility

$$T = e^{-\chi''\omega L/c}, \quad \varphi = -\frac{\chi'\omega L}{2c}. \quad (4)$$

Here, we have used the approximation $\sqrt{1+\chi} \approx 1 + \chi/2$. The quantities T and φ are plotted in Fig. 4. This figure is plotted for $\omega_0 = 2\pi(508.33) \text{ THz}$, which is the D1 transition line of sodium [18], and $L = 1 \text{ cm}$. As can be seen from Fig. 4, for detunings close to zero, φ has the highest slope. However, in this region, T is very small.

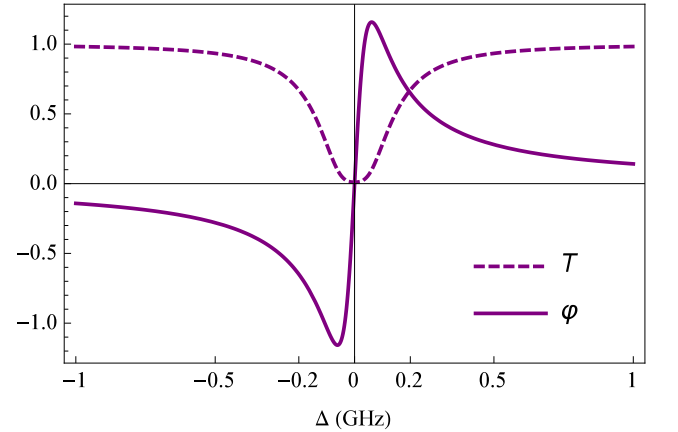


FIG. 4. The transmissivity T (dashed line) and the phase shift φ (solid line) vs. detuning Δ for the D1 transition line of sodium, $L = 1 \text{ cm}$ and $\mathcal{N} = 2.5 \times 10^{16} \text{ m}^{-3}$.

In the following section we find the optimal states to measure the transition frequency of the atoms i.e., Δ in this scheme.

III. OPTIMIZED STATES

We consider the general form of the state in the arms of the interferometer to be

$$|\psi\rangle = \sum_{k=0}^N \psi_k |N-k, k\rangle, \quad (5)$$

i.e., a pure state with the total photon number of N . We use Fisher information as the measure to quantify the metrological value of the states. According to the

Cramér-Rao bound [22] the variance in estimating a parameter, Δ in this case, using an unbiased estimate, is lower bounded by the inverse of the Fisher information $F(\Delta)$

$$\text{var}(\Delta) \geq 1/F(\Delta). \quad (6)$$

Here, we are considering photon number detection in the output modes, thus we are using classical rather than quantum Fisher information. The Fisher information represents the amount of information about Δ contained in the measurement results. It is given as

$$F(\Delta) = \sum_{n_1, n_2} \frac{1}{P_{n_1, n_2}(\Delta)} \left(\frac{\partial P_{n_1, n_2}(\Delta)}{\partial \Delta} \right)^2, \quad (7)$$

where $P_{n_1, n_2}(\Delta)$ is the probability of detecting n_1 and n_2 photons in each of the output ports.

Considering the state given in Eq. (5), applying the atom cell transformation given in Eq. (3) on the first mode, and the last 50/50 beam splitter of the interferometer on both modes, we obtain

$$\begin{aligned} P_{n_1, n_2}(\omega) = & \sum_{k=0}^{n_1+n_2} \sum_{k'=0}^{n_1+n_2} \sum_{u=n_2-k}^{n_2} \sum_{v=n_2-k'}^{n_2} \psi_k \psi_{k'}^* \frac{n_1! n_2! (N-n_1-n_2)!}{\sqrt{k! k'! (N-k)! (N-k')!}} \left(\frac{1}{2}\right)^{n_1+n_2} (-1)^{k-n_2} \\ & \times \binom{N-k'}{N-n_1-n_2} \binom{N-k}{N-n_1-n_2} \binom{n_1+n_2-k}{u} \binom{n_1+n_2-k'}{v} \binom{k}{k+u-n_2} \binom{k'}{k'+v-n_2} \\ & \times (1 - e^{-\omega L \chi''/c})^{N-n_1-n_2} e^{i\omega \chi' L(k-k')/(2c)} e^{-\omega L \chi''(2n_1+2n_2-k-k')/(2c)}, \end{aligned} \quad (8)$$

where $\omega = \Delta + \omega_0$ is the frequency of the photons in the input state. Note that we have only considered the loss due to the atomic ensemble. More generally there might be additional loss in the system which we don't consider here. Because we are quantifying the metrological value of the states via the Fisher information, we regard the optimal states to be those which maximize the Fisher information. We have found the optimal values of ψ_k numerically using the particle swarm optimization (PSO) algorithm.

In the PSO algorithm a swarm of particles search the space of ψ_k coefficients for those that maximize the Fisher information. Each particle has a velocity \vec{v} and position \vec{x} which are updated to \vec{v}' and \vec{x}' according to its best previous position \vec{x}_ℓ , and the best position of the entire swarm \vec{x}_g as [23]

$$\begin{aligned} \vec{x}' &= \vec{x} + \vec{v}', \\ \vec{v}' &= \chi [\vec{v} + c_g r_g (\vec{x}_g - \vec{x}) + c_\ell r_\ell (\vec{x}_\ell - \vec{x})]. \end{aligned} \quad (9)$$

Here, r_g and r_ℓ are uniform random numbers in the interval $[0, 1]$, and χ , c_g and c_ℓ are constants. In our simulations, we used $\chi = 0.729$, $c_\ell = c_g = 2.05$ with 10 particles and 100 iterations.

We have found that the optimal state for a specific type of atoms, only depends on the product of the number density of atoms and cell length, $\mathcal{N}L$. This can be

explained in the following way. In Eqs. (4) and (8), we have $\omega \chi' L$ and $\omega \chi'' L$ which can be written as

$$\omega \chi L = \omega L (\chi' + \chi'') = \frac{2\mathcal{N}L\mu^2\omega_0}{\hbar\varepsilon_0\gamma_s} \frac{(\Delta/\gamma_s + i)(1 + \Delta/\omega_0)}{1 + (\Delta/\gamma_s)^2}. \quad (10)$$

For a given type of atom the multiplying factor at the front can only be varied via \mathcal{N} or L . The other parameters, μ , ω_0 and γ_s can be varied by changing the type of atom. These parameters affect the variation of $\omega \chi$ in three ways:

1. They change the multiplicative factor at the front. As that factor can also be changed by varying \mathcal{N} or L , that does not give any qualitatively different results than simply changing \mathcal{N} or L .
2. The parameter γ_s appears in the ratio Δ/γ_s , and therefore provides a scaling to the variation of $\omega \chi L$ with Δ . It therefore does not qualitatively change the results.
3. The parameter ω_0 appears in the factor $(1 + \Delta/\omega_0)$. This factor affects the variation very little, because we consider a parameter regime where $\Delta/\omega_0 \ll 1$.

In the following we keep L constant at 1 cm and discuss the two cases: $\mathcal{N} > 10^{17} \text{ m}^{-3}$ (large \mathcal{N}) and $\mathcal{N} < 10^{17} \text{ m}^{-3}$ (small \mathcal{N}).

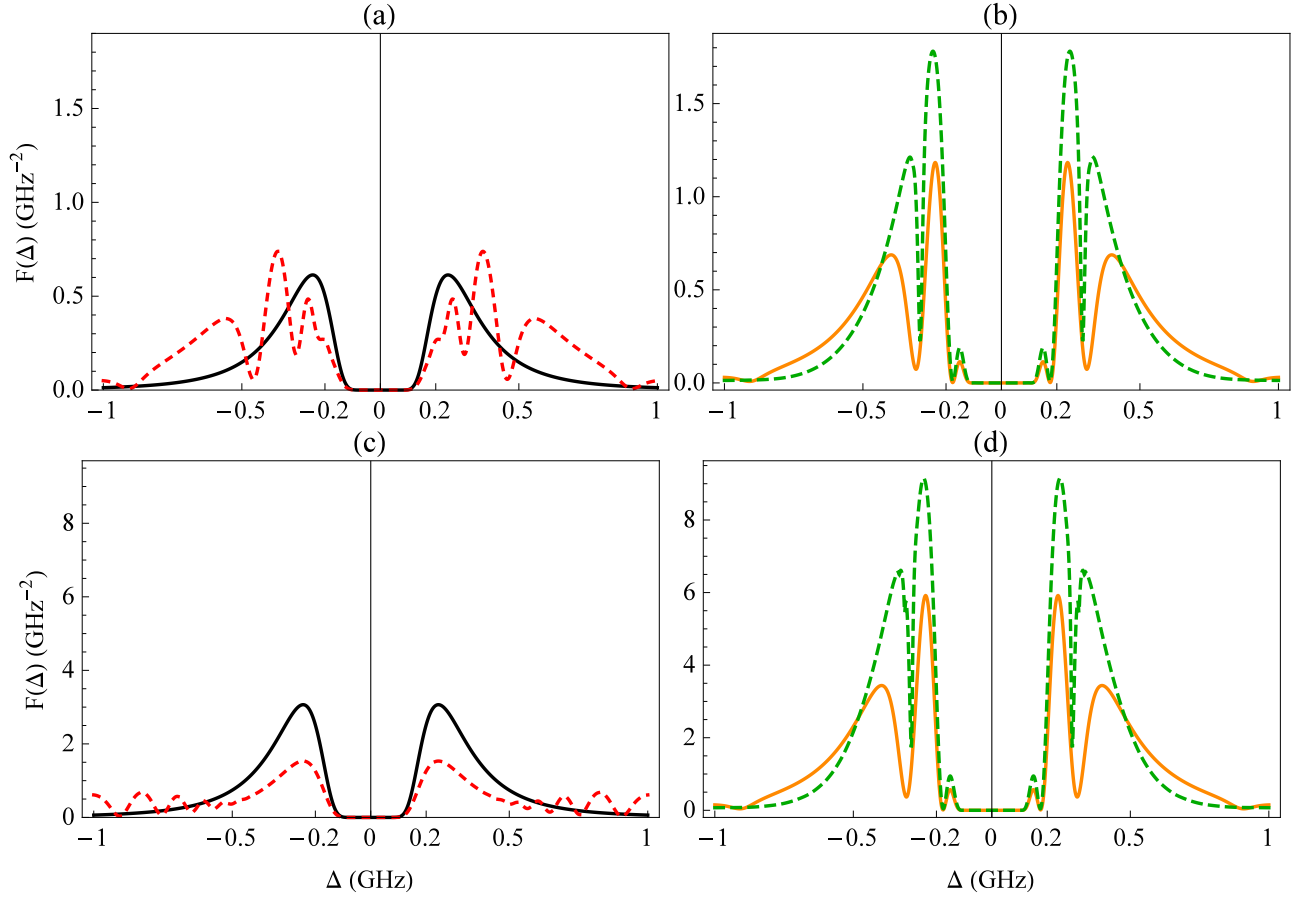


FIG. 5. Fisher information $F(\Delta)$ versus detuning Δ for $N = 2$ photons (upper row) and $N = 10$ (lower row). Solid-black line: N independent single photons $|1, 0\rangle^{\otimes N}$. Dashed-red line: N -photon NOON state $(|N, 0\rangle + |0, N\rangle)/\sqrt{2}$. Dashed-green line: N -photon optimal state. Solid-orange line: N copies of single-photon NOON states $(|1, 0\rangle + |0, 1\rangle)/\sqrt{2}$.

A. Large \mathcal{N}

For $\mathcal{N} > 10^{17} \text{ m}^{-3}$, we have found that numerically optimized states of the form given in Eq. (5) perform better than NOON states and independent single photons. In Fig. 5 we have compared the Fisher information of the N -photon optimal state, N independent single photon states $|1, 0\rangle^{\otimes N}$, N copies of a single-photon NOON state $(|1, 0\rangle + |0, 1\rangle)/\sqrt{2}$, and an N -photon NOON state $(|N, 0\rangle + |0, N\rangle)/\sqrt{2}$. This figure is plotted for $N = 2$ (upper row) and $N = 10$ (lower row). In this figure, we have used $\omega_0 = 2\pi(508.332) \text{ THz}$, which is the transition frequency of the D1 line of sodium [18], and an atom density of $\mathcal{N} = 2.5 \times 10^{17} \text{ m}^{-3}$.

Figure 5 shows that, even for $N = 2$, the enhancement obtained by optimal states is significant. For larger photon numbers, as is shown in the graphs for $N = 10$, there is no further significant improvement in the enhancement of the optimal states. Moreover, the optimal states with high photon numbers are not experimentally achievable with the current technology. On the other hand, it may be possible to generate the optimal states for $N = 2$ with

a scheme similar to the one proposed in Ref. [11].

Note that, close to resonance, for copies of single-photon NOON states the maximum peak is higher than for independent single photons and N -photon NOON states. This is as would be expected, since single-photon NOON states are the least sensitive NOON states to loss. From Fig. 5(c), we see that ten-photon NOON states perform worse than independent single photons close to resonance. However, far from resonance, their Fisher information is even higher than the numerically obtained optimal states. The reason why this is possible is that the optimal states are only optimal in the sense of giving the largest maximum Fisher information, but it is possible for other states to have larger Fisher information for detunings where the optimal states do not give their maximum Fisher information. On the other hand, as can be seen in Fig. 5(a), two-photon NOON states are less sensitive to loss (compared to ten-photon NOON states), and close to resonance they perform better than independent single photons.

The other thing to note from Fig. 5 is that to be able to work in the region with maximum Fisher information we need to have prior knowledge of the detuning. This

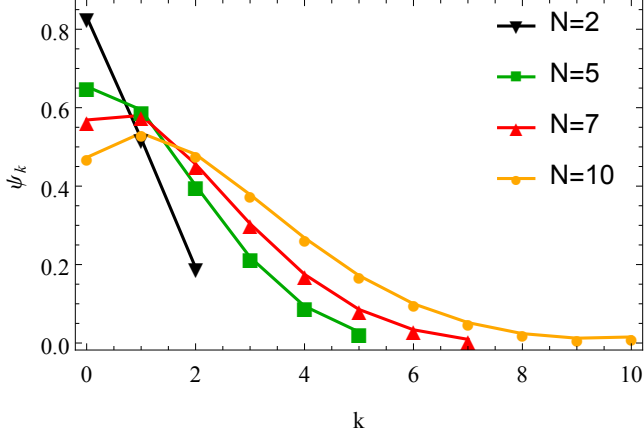


FIG. 6. Coefficients ψ_k of the optimal states for number density of atoms $\mathcal{N} = 2.5 \times 10^{17} \text{ m}^{-3}$ for four values of the total photon number N .

is because the peaks of maximum Fisher information are quite narrow. In other words this scheme could be used to measure hyperfine splitting of atomic levels, or measure external effects, such as magnetic field, on the transition frequency of atoms.

In Fig. 6 we have plotted the values of the coefficients of the optimal states, ψ_k in the superposition (5), for a range of photon numbers from $N = 2$ to $N = 10$. This figure shows that the optimal states have higher amplitudes for the terms with higher photon numbers in the arm that contains the atomic ensemble. That is, when there are more photons in the arm with the ensemble, they are more likely to be lost, giving more information about Δ .

B. Small \mathcal{N}

For smaller values of \mathcal{N} than considered in the previous subsection, the range of the phase shift is smaller (see Fig. 7). In this case, the optimal state is N independent single photons, $|1, 0\rangle^{\otimes N}$. Having all the photons in the upper arm, only the loss is being probed, and no information is being obtained from the phase shift. The phase shift must be significant so that we can take advantage of interferometric schemes in spectroscopy. Surprisingly for $\mathcal{N} = 2.5 \times 10^{16} \text{ m}^{-3}$ the maximum of the Fisher information for N independent single photons is even higher than the maximum of the Fisher information for the N -photon numerically optimized states with a larger number density of atoms which were considered in the previous subsection (see Fig. 8).

This could be understood from the variation of the transmissivity T and phase shift φ with \mathcal{N} , shown in Fig. 7. For smaller values of \mathcal{N} the range of the phase shift is also smaller, which eliminates the advantage in

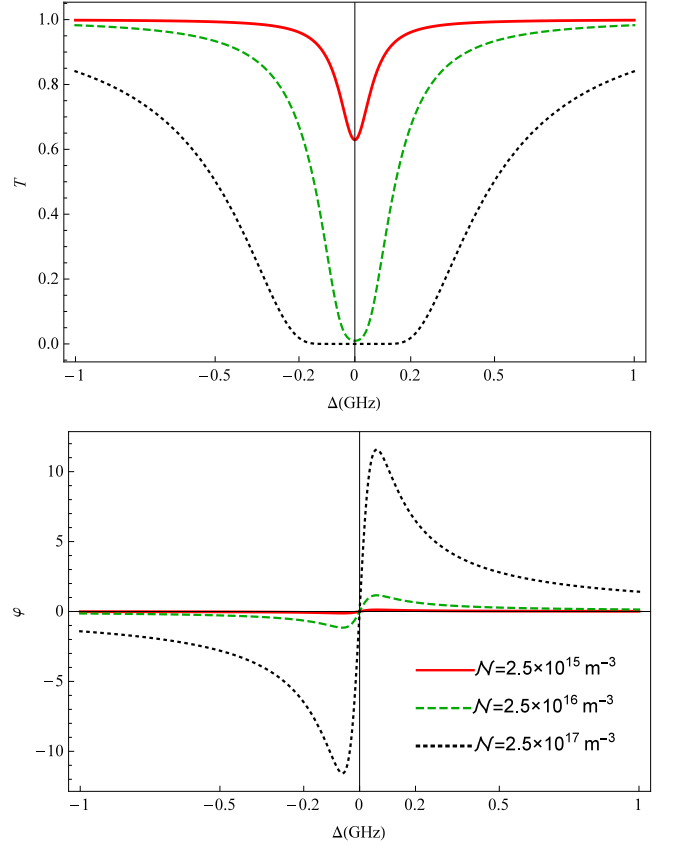


FIG. 7. Transmissivity T and phase shift φ versus Δ , for a range of values of number density of atoms \mathcal{N} . Solid-red line: $\mathcal{N} = 2.5 \times 10^{15} \text{ m}^{-3}$. Dashed-green line: $\mathcal{N} = 2.5 \times 10^{16} \text{ m}^{-3}$. Dotted-black line: $\mathcal{N} = 2.5 \times 10^{17} \text{ m}^{-3}$.

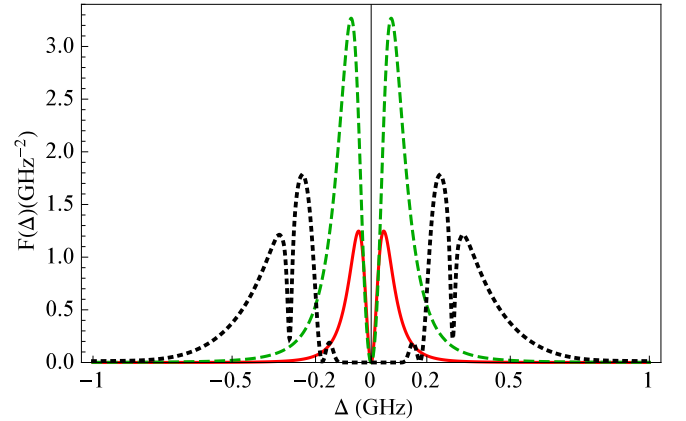


FIG. 8. Fisher information versus Δ for total number of photons $N = 2$, for the optimal states of a range of number densities of atoms \mathcal{N} . Solid-red line: N independent single photons with $\mathcal{N} = 2.5 \times 10^{15} \text{ m}^{-3}$. Dashed-green line: N independent single photons with $\mathcal{N} = 2.5 \times 10^{16} \text{ m}^{-3}$. Dotted-black line: numerically optimized state with $\mathcal{N} = 2.5 \times 10^{17} \text{ m}^{-3}$.

using entangled states. In this case, the Fisher information is coming from the variation in the absorption. As \mathcal{N} is decreased further, the dip in the absorption is re-

duced which results in a smaller Fisher information. For the higher densities, there is a larger phase shift, but it is in a region where the absorption is very high.

IV. CONCLUSION

In this work we found optimal multi-photon states for measurement of the transition frequency of atoms. The scheme proposed here is an interferometric scheme with photon number detection in the output. In order to find the best states for measurement of the transition frequency, we numerically optimized for the states that provide the largest Fisher information.

For the number density of atoms we considered initially, the imposed phase on the probe is large, and it is advantageous to using information from both the absorption and the phase shift for measuring the transition frequency. In this case, the optimal state is an entangled multi-photon state. This optimal state has a large weighting on the state with all photons in the arm with the atomic ensemble. On the other hand, for a smaller number density of atoms, the phase shift imposed on the probe is small and therefore the information from the phase shift is not significant enough to give any advantage. In this case, the optimal state is independent single photons. In other words, it is advantageous to pass all

the photons through the atom cell and obtain all the information from absorption.

Surprisingly there is a value of the number density, $\mathcal{N} = 2.5 \times 10^{16} \text{ m}^{-3}$ for which N independent single photons have the highest Fisher information. This Fisher information is even higher than the Fisher information for the N -photon numerically optimized states with a larger number density of atoms. Therefore, if we have control over the number density of atoms it is better to choose this number density and probe the ensemble with independent single photons.

More generally, it would be possible to consider loss in both arms of the interferometer in addition to the atom cell. Recalculating optimal states for different situations with different amounts of losses is a possible topic for future work.

V. ACKNOWLEDGEMENTS

MKG and JPD would like to acknowledge funding from the Air Force Office of Scientific Research, The Army Research office, The National Science Foundation, and the Northrop Grumman Corporation. DWB is funded by an ARC Future Fellowship (FT100100761) and a Discovery Project (DP160102426).

-
- [1] V. Giovannetti, S. Lloyd, and L. Maccone, *Science* **306**, 1330 (2004); V. Giovannetti, S. Lloyd, and L. Maccone, *Nat. Photon.* **5**, 222, (2011).
 - [2] F. Wolfgramm, C. Vitelli, F. A. Beduini, N. Godbout and M. W. Mitchell *Nat. Photon.* **7**, 28 (2012).
 - [3] M. A. Taylor, J. Janousek, V. Daria, J. Knittel, B. Hage, H.-A. Bachor, and W. P. Bowen, *Nature Photon.* **7**, 229 (2013).
 - [4] B. C. Sanders, *Phys. Rev. A* **40**, 2417 (1989).
 - [5] H. Lee, P. Kok, and J. P. Dowling, *J. Mod. Opt.* **49**, 2325 (2002).
 - [6] M. A. Rubin and S. Kaushik, *Phys. Rev. A* **75**, 053805 (2007).
 - [7] G. Gilbert and Y. S. Weinstein, *J. Mod. Opt.* **55**, 3283 (2008).
 - [8] U. Dorner, R. Demkowicz-Dobrzanski, B. J. Smith, J. S. Lundeen, W. Wasilewski, K. Banaszek, and I. A. Walmsley, *Phys. Rev. Lett.* **102**, 040403 (2009).
 - [9] R. Demkowicz-Dobrzański, U. Dorner, B. J. Smith, J. S. Lundeen, W. Wasilewski, K. Banaszek, and I. A. Walmsley, *Phys. Rev. A* **80**, 013825 (2009).
 - [10] M. Kacprowicz, R. Demkowicz-Dobrzański, W. Wasilewski, K. Banaszek, and I. A. Walmsley, *Nat. Photon.* **4**, 357 (2010).
 - [11] H. T. Dinani and D. W. Berry, *Phys. Rev. A* **90**, 023856 (2014).
 - [12] S. Scheel, *J. Mod. Opt.* **50**, 1327 (2003).
 - [13] R. Whittaker, C. Erven, A. Neville, M. Berry, J. L. O'Brien, H. Cable and J. C. F. Matthews, *arXiv:1508.00849* (2015).
 - [14] J. D. Jackson, "Classical electrodynamics", (Wiley, 1999).
 - [15] P. J. D. Crowley, A. Datta, M. Barbieri, and I. A. Walmsley, *Phys. Rev. A* **89**, 023845 (2014).
 - [16] P. Kok, B. W. Lovett, "Introduction to optical quantum information processing", (Cambridge University Press, 2010), p. 336.
 - [17] R. G. Beausoleil and W. J. Munro and T. P. Spiller, *J. Mod. Opt.* **51**, 1559 (2004).
 - [18] D. A. Steck, Sodium D Line Data (2001), <http://steck.us/alkalidata/sodiumnumbers.pdf>
 - [19] J. R. Jeffers, N. Imoto, R. Loudon, *Phys. Rev. A* **47**, 3346 (1993).
 - [20] R. Loudon, "The quantum theory of light, (Oxford University Press, Oxford, 2001), p. 311.
 - [21] T. W. Lee, S. D. Huver, H. Lee, L. Kaplan, S. B. McCracken, C. Min, D. B. Uskov, C. F. Wildfeuer, G. Veronis, and J. P. Dowling, *Phys. Rev. A* **80**, 063803 (2009).
 - [22] S. L. Braunstein and C. M. Caves, *Phys. Rev. Lett.* **72**, 3439 (1994).
 - [23] D. Bratton and J. Kennedy, *Proceedings of the 2007 IEEE Swarm Intelligence Symposium*, p. 120 (2007).